



HAL
open science

Is winter coming? Minor effect of the onset of chilling accumulation on the prediction of endodormancy release and budbreak

Guillaume Charrier

► To cite this version:

Guillaume Charrier. Is winter coming? Minor effect of the onset of chilling accumulation on the prediction of endodormancy release and budbreak. *Physiologia Plantarum*, 2022, 174 (3), 10.1111/ppl.13699 . hal-03767573

HAL Id: hal-03767573

<https://hal.inrae.fr/hal-03767573>

Submitted on 15 Mar 2023

HAL is a multi-disciplinary open access archive for the deposit and dissemination of scientific research documents, whether they are published or not. The documents may come from teaching and research institutions in France or abroad, or from public or private research centers.

L'archive ouverte pluridisciplinaire **HAL**, est destinée au dépôt et à la diffusion de documents scientifiques de niveau recherche, publiés ou non, émanant des établissements d'enseignement et de recherche français ou étrangers, des laboratoires publics ou privés.

Copyright

SPECIAL ISSUE ARTICLE

Is winter coming? Minor effect of the onset of chilling accumulation on the prediction of endodormancy release and budbreak

Guillaume Charrier 

Université Clermont Auvergne, INRAE, PIAF, Clermont-Ferrand, France

Correspondence

Guillaume Charrier, Université Clermont Auvergne, INRAE, PIAF, 63000 Clermont-Ferrand, France.

Email: guillaume.charrier@inrae.fr

Funding information

Agence Nationale de la Recherche, Grant/Award Number: ANR-20-CE91-008; Auvergne-Rhone-Alpes Region; European Commission (Life Frostdefend), Grant/Award Number: CCA/GR/001747; INRAE - AgroEcoSystem; Pôle National de Données de la Biodiversité

Edited by M. Uemura

Abstract

The buds of perennial plants become dormant in autumn and must integrate the information related to chilling and forcing temperatures to resume their growth in spring. In many studies, the initial date for chilling accumulation (D_{CA}) is set arbitrarily using various rules resulting in high variability across studies and sites. To test the relevancy of different rules to set D_{CA} , sequential models (taking into account or not the negative effect of warm temperature) were optimized by minimizing the sums of squares between observed and predicted values for 34 endodormancy release and 77 budbreak dates for the walnut *Juglans regia* L. cv Franquette across France. Optimization of these different models highlighted that many of the D_{CA} rules, incorporating a photoperiod signal on endodormancy induction, were effective (predicted root mean square standard error less than 10 and 8 days for endodormancy onset and bud break, respectively). Furthermore, the use of functions that compute negative chilling accumulation did not improve the performance of the models. Among the different rules, the projections of the best models were explored under different climates (current climate and Representative Concentration Pathways RCP scenarios). The projections revealed a tipping point at a mean annual temperature between 13 and 15°C, beyond which the advance in ontogenic development during endodormancy does not compensate for the delay in endodormancy release. Although the physiological mechanisms driving the onset of endodormancy may be profoundly altered by global change, they appear to have minimal impact on the way current models predict dormancy and budbreak dates in walnut.

1 | INTRODUCTION

In frost-exposed environments, deciduous trees must timely adjust their phenology to anticipate unfavorable conditions during the winter period. To avoid exposure to frost events, meristems switch from an apparently active period to a “dormant” period, characterized by the inability to grow even under favorable conditions (Charrier et al., 2015). In temperate species, bud dormancy is divided into three stages depending on the inhibiting factor (Lang et al., 1987). During paradormancy, in late summer, other organs

such as apical bud or leaves inhibit meristem growth. During endodormancy, in autumn, growth is inhibited by factors intrinsic to the bud (“endo”), whereas during ecodormancy, in late winter-early spring, growth is limited by environmental factors (“eco”). Different phenological stages are visible during the transition from growth to dormancy (e.g. growth cessation, leaf fall, lignification, or bud set), whereas others are cryptic (e.g. endodormancy induction and release). Observation of the succession of phenological stages is therefore difficult, which makes prediction in a changing environmental context even more challenging.

Various factors control dormancy, including its depth (Faust et al., 1997): metabolic activity, morphological changes, and hormonal balance (e.g. auxine during paradormancy, abscisic acid during endodormancy; Beauvieux et al., 2018; Horvath et al., 2003). The interaction between these factors and environmental cues triggers the transition between dormancy stages. In late summer, the induction of endodormancy is mainly triggered by the decreasing photoperiod and low nighttime temperature (Maurya & Bhalerao, 2017). The deposition of callose on plasmodesmata within the shoot apical meristem has been suggested to block the coordination of these cells to resume growth (Rinne et al., 2001). In autumn, endodormancy release is under the control of decreasing temperature (Arora et al., 2003; Welling et al., 2002). Low temperature would promote the 1,3 β -D-glucanase activity that would hydrolyze callose deposits (Rinne et al., 2001). After the release of endodormancy, cryptic growth of ecodormant buds progresses under the control of warm temperature, in most species, eventually modulated by photoperiod in photosensitive species, such as late successional species (Basler & Körner, 2012).

In the context of global change, temperature would be expected to change at a given location, whereas photoperiod signals would remain similar, thus jeopardizing the regulation of phenological stages. Phenological processes would be affected in a complex manner (e.g. budbreak may be either delayed, due to the effect of warmer temperature during the endodormancy induction or release, or hastened, if warming occurs during the ecodormancy stage; Beil et al., 2021). The induction of endodormancy, under the dual control of cold temperature and short photoperiod could be particularly disturbed.

Since the first empirical model describing the relationship between temperature and plant development, through the concept of thermal-time (Réaumur, 1735), budbreak and flowering models have only computed the accumulation of growth-effective temperature (i.e. growth degree days GDD). As the starting point is set close to the coldest time of the year (e.g. January 1st or July 1st usually chosen for convenience in the northern and southern hemispheres, respectively), these models provide relatively accurate results. However, this type of model is not effective in regions with warmer winters, where temperate crop species have been introduced (e.g. in North Africa, the Middle East or South America; Balandier et al., 1993). In this context, temperate perennial crops exhibit a lack of chilling and insufficient endodormancy release (Weinberger, 1950). The process of endodormancy, and the related chilling accumulation, was therefore introduced into the models (Vegis, 1964; Weinberger, 1956). Different chilling accumulation functions have been developed, depending on the species. An important difference is the consideration of a delaying effect on endodormancy release for warm temperature (e.g. Utah model; Richardson et al., 1974) or not (e.g. Chilling hours; Weinberger, 1967). In recent decades, naturally growing trees have also been affected by a reduction in chilling exposure throughout the winter, increasing interest in the endodormancy stage (Beil et al., 2021; Pagter et al., 2015).

Phenological models using environmental variables as inputs have been developed to simulate the endodormancy release and budbreak

dates (Caffarra, Donnelly, Chuine, & Jones, 2011a; Chuine et al., 2016). In perennial plants, the completion of one stage is concomitant with the onset of the following one (Hänninen & Tanino, 2011). However, the initial date for chilling accumulation (D_{CA}) is usually set arbitrarily with various rules resulting in a large variability between studies (from late summer to late autumn). Here, I explored four different concepts of D_{CA} to assess their effect on current and future predictions of endodormancy release and budbreak:

- fixed D_{CA} ,
- variable D_{CA} through a simple climatic threshold,
- variable D_{CA} through a mathematic function using temperature as the only variable,
- variable D_{CA} through a mathematic function using interacting variables (temperature and photoperiod).

Based on what is known in the induction of endodormancy, data from 1975 until 2019 from different orchards across France for *Juglans regia* cv Franquette, were used along with different computations to simulate effects of the onset of chilling accumulation D_{CA} on the predictive accuracy of endodormancy release and budbreak dates. Specifically, I tested whether the use of dynamic D_{CA} could account for the delaying effect of warm temperature on endodormancy release by comparing positive and positive/negative chilling functions. In a second step, the best models were evaluated to predict endodormancy release and budbreak in future climate scenarios for France.

2 | MATERIAL AND METHODS

2.1 | Dormancy depth and endodormancy release

Endodormancy release dates were measured using the one-node-cutting “forcing” test of Rageau (1982). Sampling was performed every 3 weeks from October to March and 48 one-node cuttings were prepared per sampling date. On each sampling date, one-year-old stems were sampled from five individual trees and cut into 7-cm long pieces, bearing only one node at the top or within 1 cm below the upper end, for terminal and axillary buds, respectively. For axillary buds, the top of the cutting was covered with paraffin to prevent desiccation. If present, other buds were cut from the cutting with a razor blade to avoid correlative inhibitions (Dennis, 2003). The bases of the cuttings were immersed in tap water and changed weekly. Forty-eight cuttings were exposed to forcing conditions (i.e. 16/8 h day/night and 25°C constant) and observed individually every 3 days. The mean time to budbreak (stage 09 BBCH; Meier, 2001) was computed as the average of the individual time to budbreak for each of the 48 cuttings. After endodormancy release, buds of *J. regia* cv Franquette break after 20 days or less under optimal conditions (Charrier et al., 2011; Mauget, 1980). Endodormancy release dates were obtained by linear interpolation between the two dates giving a time to budbreak greater than (or equal to) and less than (or equal to) 20 days, respectively.

TABLE 1 Site and dataset descriptions

Location	Elevation (m asl.)	Latitude (°)	Longitude (°)	Mean annual temperature (°C)	Minimum temperature (°C)	Absolute minimum temperature (°C)	Number of freezing events	First frost (autumn) DOY	Last frost (spring) DOY	Number of observations			
										Endodormancy release		Budbreak	
										Dataset 1 (C/V)	Dataset 2 (C/V)	Dataset 1 (C/V)	Dataset 2 (C/V)
Arsins Island	22	44.792	-0.577	14.29	9.47	-5.47	23.77	305	67	1/0	1/0	0/0	0/0
Balandran	69	43.758	4.516	16.90	12.00	-3.78	14.5	340	50	1/1	1/1	0/0	0/0
Chatte	304	45.143	5.282	13.62	8.15	-9.39	61.7	308	102	0/0	0/0	12/11	11/12
Creyse	115	44.887	1.597	14.65	8.52	-8.50	52.4	309	104	0/0	0/0	13/12	12/13
Crouël	340	45.779	3.142	13.25	9.26	-11.51	59.6	302	108	13/12	12/13	4/4	4/4
Orcival	1150	45.683	2.842	12.92	7.72	-12.13	97.4	291	126	1/1	1/1	1/0	1/0
Terrasson	90	45.136	1.300	14.61	8.96	-9.69	47.4	311	100	1/1	1/1	1/0	1/0
Theix	945	45.706	3.021	9.70	6.22	-15.11	100.3	282	129	1/1	1/1	1/0	1/0
Toulence	22	44.557	-0.263	15.38	10.56	-6.09	25.9	325	74	0/0	0/0	9/9	9/9

Note: C/V refers to the amount of observation in the calibration and validation dataset, respectively.

2.2 | Budbreak dates

Budbreak dates were monitored every 2–3 days at the different sites on five individual trees until 50% of buds reached the BBCH stage 09. The different sites and number of annual observations are shown in Table 1.

2.3 | Climatic data

The models were fitted using the daily average and minimum temperatures observed by the weather stations, mostly located in the same orchard or within a 10 km distance (Table 1). For prediction, temperatures, calculated according to the CNRM-ALADIN52 model and corrected by a Q-Q method (Déqué et al., 2007), were used from 8462 sites across France (Safran grid at 64 km² spatial resolution; MétéoFrance). Four datasets were used as input variables: the reference period (1950–2005) and three climate scenarios (Representative Concentration Pathways RCP 2.6, RCP 4.5, and RCP 8.5) for the future period: short-term (2006–2051) and long-term (2051–2100). For each site, day length was computed as a function of latitude and day of the year.

2.4 | Endodormancy induction and onset of chilling accumulation

The initial date for chilling accumulation (D_{CA}) was computed using different functions (see Table S1):

1. Fixed date as a day of the year (DOY).
2. Flexible date based on the threshold values reached by the minimum temperature (T_{min}), the mean temperature (T_{mean}), the first frost (FF) or the photoperiod.

3. Date of minimum chilling units (CU_{min}) computed according to the Utah model (originally developed on *Prunus persica* L. Batsch), which computes the negative chilling effect for temperatures above 16°C (Richardson et al., 1974). Daily CUs were summed from DOY 182 until DOY 365 using the Utah_Model function (ChillIR package; Luedeling, 2019) as follows:

$$CU[T_{mean}] = \begin{cases} 0 & \text{if } T_{mean} < 1.4 \\ 0.5 & \text{if } 1.5 < T_{mean} < 2.4 \\ 1 & \text{if } 2.5 < T_{mean} < 9.1 \\ 0.5 & \text{if } 9.2 < T_{mean} < 12.4 \\ 0 & \text{if } 12.5 < T_{mean} < 15.9 \\ -0.5 & \text{if } 16 < T_{mean} < 18 \\ -1 & \text{if } T_{mean} > 18 \end{cases} \quad (1)$$

with T_{mean} the daily mean temperature.

4. Predicted leaf fall dates (BBCH 97) were computed according to the thermal (LFT) and photothermal (LFPT) models developed by Delpierre et al. (2009) for *Quercus* and *Quercus + Fagus*, respectively. Below a critical photoperiod DL_{start} and for a temperature colder than a threshold T_b , the variable R_{sen} , modulated by a photoperiod function in the case of the LFPT model, is summed daily up to a critical value (Y_{crit}), corresponding to the leaf fall date and considered as D_{CA} . Both LFT and LFPT models were computed using the original or optimized parameter sets: LF(P) T_{ori} and LF(P) T_{adj} , respectively.

$$R_{sen}[T_{mean}; DL] = \begin{cases} 0 & \text{if } DL \geq DL_{start} \\ 0 & \text{if } T_{mean} \geq T_b \\ [T_{mean} - T_b]^2 \times \left(1 - \frac{DL}{DL_{start}}\right)^y & \text{if } T_{mean} < T_b \end{cases} \quad (2)$$

with T_{mean} the daily mean temperature and DL the photoperiod. The parameter γ was set to 0 and 2 for LFT and LFPT models, respectively.

5. The endodormancy induction state (DS) was computed according to the DORMPHOT model developed for *Betula pubescens* Ehrh. by Caffarra, Donnelly, Chuine, and Jones (2011a). The two sigmoidal response functions to low temperature and photoperiod interact to compute DS. When the sum of daily DS reaches D_{crit} , the date is reported as D_{CA} . Both the original (DP_{ori}) and optimized (DP_{adj}) parameter sets were used.

$$DS[T_{\text{mean}}; DL] = \frac{1}{1 + e^{aD(T_{\text{mean}} - bD)}} \times \frac{1}{1 + e^{10(24 - DL - DL_{\text{crit}})}} \quad (3)$$

with T_{mean} the daily mean temperature, DL the photoperiod, aD a coefficient for the effect of temperature, bD a critical temperature, and DL_{crit} a critical photoperiod.

2.5 | Endodormancy release and budbreak

From the D_{CA} , the effect of chilling temperature was simulated according to the inverse of the function used for forcing accumulation in the original studies from Richardson et al. (1974). This function was defined as the best function predicting endodormancy release dates in walnut trees, although it does not take into account the negation of chilling at warm temperatures (Charrier, Chuine, et al., 2018a; Chuine et al., 2016). According to the sequential paradigm, the date at which the sum of CU reaches the critical CU_{crit} threshold (arbitrary chilling units, CU) is the date of endodormancy release (D_{ER}), or the transition from endodormancy to ecodormancy:

$$CU[T_{\text{mean}}] = \text{Max}[\text{Min}(T_{\text{high}} - T_{\text{mean}}; T_{\text{high}} - T_{\text{low}}); 0] \quad (4)$$

with $CU(t)$ the chilling unit on day t , T_{high} the temperature above which $CU(t)$ is 0 and T_{low} the temperature below which $CU(t)$ is maximum; $CU(t)$ is linear between T_{low} and T_{high} .

Alternatively, the smoothed-Utah function, a smoothed version of the Utah function proposed by Richardson et al. (1974), takes into account the negation of chilling on warm days (Bonhomme et al., 2007).

$$CU[T_{\text{mean}}] = \begin{cases} \frac{1}{1 + e^{-\frac{T_{\text{mean}} - T_{m1}}{T_{\text{opt}} - T_{m1}}}} & \text{if } T_{\text{mean}} > T_{m1} \\ \frac{0.5(T_{\text{mean}} - T_{\text{opt}})^2}{(T_{m1} - T_{\text{opt}})^2} & \text{if } T_{m1} < T_{\text{mean}} < T_{\text{opt}} \\ 1 - \frac{(1 - \min)\frac{(T_{\text{mean}} - T_{\text{opt}})^2}{2(T_{n2} - T_{\text{opt}})^2}}{2} & \text{if } T_{\text{opt}} < T_{\text{mean}} < T_{n2} \\ \min + \frac{1 - \min}{1 + e^{-\frac{T_{n2} - T_{\text{mean}}}{T_{n2} - T_{\text{opt}}}}} & \text{if } T_{n2} < T_{\text{mean}} \end{cases} \quad (5)$$

with $CU(t)$ the chilling unit at day t , T_{opt} the optimal temperature for chilling, T_{m1} the slope of the cold efficiency at a colder temperature than T_{opt} , T_{n2} the temperature warmer than T_{opt} , which has half the efficiency of T_{opt} to release endodormancy; min the effect of warm temperature to remove previously accumulated CU.

Ontogenetic development during the ecodormancy stage was modeled using a sigmoid function (Caffarra, Donnelly, Chuine, & Jones, 2011a). FU was summed daily from D_{ER} until it reached the critical threshold FU_{crit} (arbitrary forcing units, FU), considered as the budbreak date (D_{BB}).

$$FU[T_{\text{mean}}] = \frac{1}{1 + e^{-\text{slp}(T_{\text{mean}} - T_{50})}} \quad (6)$$

with $FU(t)$ the forcing unit at day t , slp the slope of the function at the temperature, inducing half of the maximal apparent growth rate T_{50} .

2.6 | Model calibration depending on the onset of chilling accumulation

For a given D_{CA} rule, the date of endodormancy release was calibrated first and the best set of parameters was used to calibrate the bud break date. This sequential procedure was chosen to ensure that the date of endodormancy release would be realistic, which is not the case when a model is optimized only on budbreak dates (Chuine et al., 2016). For the endodormancy release model, in addition to the parameters defining D_{CA} (between 1 [DOY and photoperiod] and 4 [LFT, LFPT, and DORMPHOT]; Table S2), three or five parameters were optimized for the reverse Richardson and the smoothed-Utah functions, respectively. For the ecodormancy model, one parameter was optimized: FU_{crit} corresponding to the sum of forcing units for bud break. The endodormancy model used to predict D_{ER} was the best from the previous step and the other parameters (slp and T_{50}) set to the values described in Charrier, Chuine, et al. (2018a).

The nls function (using Gauss-Newton algorithm, R version 3.6.2; R development Core Team, 2019) was used to minimize the sums of squares between the observed and predicted values with different sets of starting values at the minimum, average, and maximum ranges of realistic parameter values. In order to maximize the variability within the datasets. The calibration was performed using approximately half of the observation per site for the calibration dataset and the other half for the validation dataset. Two independent calibration procedures were performed using at least one observation per site for the calibration (Tables S3 and S4). Most of the observations used in the calibration dataset #1 were used for validation in the second calibration and vice versa.

The quality of the fit and predictive ability of the models in relation to the D_{CA} were assessed for calibration and validation datasets by several indexes independently for D_{ER} and D_{BB} : Efficiency (Eff), Root Mean Square Error (RMSE), Predictive Root Mean Square Error (RMSEP), and Akaike Index Criterion (AIC_C ; Akaike, 1974):

$$\text{Eff} = 1 - \frac{\sum_{i=1}^n (\hat{y}_i - y_i)^2}{\sum_{i=1}^n (\hat{y}_i - \bar{y})^2} \quad (7)$$

with \hat{y}_i the predicted values for an observation i , y_i the observed values for an observation i and \bar{y} the mean of observed values.

$$\text{RMSE}(P) = \sqrt{\frac{\sum_{i=1}^n (\hat{y}_i - y_i)^2}{n}} \quad (8)$$

with \hat{y}_i the predicted values for an observation i and y_i the observed values for an observation i .

$$\text{AIC}_C = 2n \left[\log(\text{RMSE}) + \frac{k}{n-k-1} \right] \quad (9)$$

with k the number of parameters, n the number of observations.

2.7 | Correlations between simulated and climate variables

A subset of the more efficient rules was selected based on their relative accuracy for the two datasets and the predicted dates (RMSE, RMSEP, and $\text{AIC}_C < 110\%$ of the minimum value for more than 9 of the 12 indexes shown on Tables 2 and 3). Parameters were optimized on the whole dataset for these relevant models and used to simulate D_{CA} , D_{ER} , and D_{BB} from 1950 to 2005 per site (8462 sites at 64 km² spatial resolution). Correlations between the mean D_{CA} , D_{ER} , and D_{BB} per site (8462 sites at 64 km² spatial resolution) and mean annual temperature were fitted by minimizing the sums of squares using a non-linear regression procedure (function nls in R). Different functions were tested: linear, sigmoid, exponential, power, second, third, or fourth degree polynomial) and selected according to RMSE and AIC_C .

3 | RESULTS

3.1 | Dormancy stages

During the induction stage of endodormancy, the time to budbreak generally increased by 20 days between August and October (onset of endodormancy) and reaches a maximum value (50–80 days: maximum endodormancy depth) between October and December (Figure 1A). The endodormancy release was observed when the time to breakbud gradually decreased to 20 days. The transition from endodormancy to ecodormancy was marked by a breakpoint in the curves between mid-December and mid-February. Significant linear correlations were observed between the onset of endodormancy and the date of maximum depth of dormancy ($F_{1,15} = 11.09$; $P = 0.005$; Figure 1B) and between the date of maximum depth of

dormancy and the date of endodormancy release (D_{ER} ; $F_{1,29} = 5.21$; $P = 0.030$; Figure 1C). However, no correlation was observed between the onset of endodormancy and D_{ER} ($F_{1,15} = 0.79$; $P = 0.387$; Figure 1D).

3.2 | Effects of D_{CA} on endodormancy release date

With the exception of a few irrelevant rules, the use of different rules to compute the initial date for chilling accumulation (D_{CA}) had a relatively small effect on the accuracy of D_{ER} prediction (Table 2). The use of a positive chilling function was overall more efficient than functions that take into account the delaying effect of warm temperature (positive and negative). Approximately 75% of the rules tested returned RMSE-values within a range of 2–3 days: between 11.5 and 13.3 days and between 7.2 and 9.5 days for datasets #1 and #2, respectively. However, the uses of first frost (FF) and the Utah model ($\text{CU}_{\text{min-ori}}$) were not effective for both datasets. Only four rules provided efficiencies higher than 0.5 for dataset #1 (LFT_{adj} and DP_{adj}, positive only, and positive and negative for both), while 11 rules had similar performance for dataset #2. The predictive ability was relatively good for most of the D_{CA} , with 75% of the RMSEP between 8.3 and 11.6 days and between 12.9 and 14.4 days for datasets #1 and #2, respectively. Finally, only a few rules returned values below 125% of the minimum for RMSE, RMSEP, and AIC_C in both datasets: Photoperiod and LFPT_{adj} (positive only), $\text{CU}_{\text{min-adj}}$ (positive and negative), LFPT_{ori}, DP_{ori}, and DP_{adj} (positive only and positive and negative). By increasing the stringency to 110%, only DP_{adj} (positive only) could be considered more accurate and robust for all indices (RMSE, RMSEP, and AIC_C) and both datasets.

3.3 | Effects of D_{CA} on budbreak date

The accuracy of the fits was slightly better for the budbreak date (D_{BB}) than for the D_{ER} (Table 3), although the effect of the different rules on the D_{BB} was relatively similar to that observed for the D_{ER} . The positive chilling function was more effective than the positive and negative functions. For most of the D_{CA} , 75% of the RMSEs were within a 2–3 day range: between 7.4 and 9.6 days and between 6.8 and 8.6 days for datasets #1 and #2, respectively. The uses of FF and $\text{CU}_{\text{min-ori}}$ were also less efficient. Most rules provided efficiencies higher than 0.5 for datasets #1 and #2 (17 and 18, respectively). The predictive ability was less than 1 week for most of the D_{CA} , with 75% of the RMSEP between 6.7 and 9.3 days and between 6.9 and 8.2 days for datasets #1 and #2, respectively. Most rules returned values below 125% of the minimum for RMSE, RMSEP and AIC_C for both datasets, with the exception of FF and $\text{CU}_{\text{min-ori}}$. By increasing the stringency to 110%, several rules remained accurate and robust: DOY, photoperiod, LFPT_{adj} (positive only), LFT_{ori} (positive and negative), LFPT_{ori}, and DP_{ori} (positive only and positive and negative).

TABLE 2 Performance of different rules to set the onset of chilling accumulation D_{CA} on the prediction of endodormancy release dates (D_{ER}) for two different calibration datasets

Onset of chilling accumulation D_{CA}	Chilling effect	Dataset 1						Dataset 2				
		k	n	Eff	RMSE	AIC _C	RMSEP	n	Eff	RMSE	AIC _C	RMSEP
Day of year	Positive only	4	18	0.497	12.16	97.9	11.57	17	0.600	8.14	82.6	13.58
	Positive and negative	6	18	0.468	12.50	102.9	11.49	17	0.534	9.51	88.6	14.26
Mean temp	Positive only	4	18	0.457	12.63	99.3	11.18	17	0.427	9.36	84.0	13.46
	Positive and negative	6	18	0.403	13.24	105.0	11.00	17	0.293	10.39	91.6	19.22
Min temp	Positive only	4	18	0.456	12.64	99.3	10.47	17	0.405	9.53	84.7	13.50
	Positive and negative	6	18	-2.374	12.92	104.1	9.32	17	-1.517	9.40	88.2	14.31
First frost	Positive only	3	18	0.002	17.12	108.3	13.30	17	-0.156	13.28	93.9	17.76
	Positive and negative	5	18	0.257	14.78	106.9	12.58	17	0.175	11.22	92.2	15.58
Photoperiod	Positive only	4	18	0.484	12.31	98.4	10.31	17	0.602	7.80	77.8	13.90
	Positive and negative	6	18	0.295	14.39	108.0	12.85	17	0.519	8.57	85.0	14.31
CU _{min} ori	Positive only	3	18	0.232	15.02	103.5	12.82	17	0.174	11.23	88.2	16.21
	Positive and negative	1	18	-5.696	44.35	138.5	47.87	17	-16.245	51.32	135.9	40.07
CU _{min} adj	Positive only	7	18	0.445	12.77	105.7	10.56	17	0.303	10.28	93.2	13.36
	Positive and negative	9	18	0.400	13.27	111.1	8.30	17	0.506	8.68	91.5	13.48
Leaf fall thermal ori	Positive only	3	18	0.435	12.88	98.0	10.30	17	0.445	9.21	81.5	13.98
	Positive and negative	5	18	0.439	12.83	101.9	10.12	17	0.456	9.11	85.1	14.19
Leaf fall thermal adj	Positive only	6	18	0.517	11.91	101.2	10.77	17	0.602	7.79	81.8	13.59
	Positive and negative	8	18	0.521	11.86	105.0	13.29	17	0.606	7.75	85.6	14.43
Leaf fall photothermal ori	Positive only	3	18	0.404	13.23	99.0	8.54	17	0.573	8.08	77.0	13.98
	Positive and negative	5	18	0.387	13.42	103.5	8.99	17	0.611	7.71	79.4	14.24
Leaf fall photothermal adj	Positive only	6	18	0.449	12.73	103.6	8.72	17	0.595	7.86	82.1	14.15
	Positive and negative	8	18	0.489	12.26	106.2	10.67	17	0.618	7.64	85.1	14.06
DORMPHOT ori	Positive only	3	18	0.445	12.77	97.7	9.08	17	0.560	8.20	77.5	13.86
	Positive and negative	5	18	0.415	13.11	102.6	9.55	17	0.485	8.87	84.2	14.38
DORMPHOT adj	Positive only	7	18	0.526	11.79	102.8	8.45	17	0.580	7.72	83.5	12.90
	Positive and negative	9	18	0.549	11.51	105.9	10.35	17	0.661	7.20	85.1	14.27

Note: RMSE, RMSEP, and AIC_C lower than 110% of the minimum RMSE or RMSEP are indicated in bold. D_{CA} were either fixed (DOY) or computed according to: Date of first frost (FF), minimum temperature (T_{min}), mean temperature (T_{mean}), photoperiod, minimum chilling unit (CU_{min}), leaf fall using temperature (LFT) or temperature and photoperiod (LFPT) and dormancy induction state using the DORMPHOT model (DP). The terms ori and adj refer to the original published version or adjusted to the data, respectively. Chilling effect were only positive, using the reverse Richardson function, or negative at warm temperature, using the smoothed Utah function. k is the number of fitted parameters and n the number of data used to fit the model.

TABLE 3 Performance of different rules to set the onset of chilling accumulation (D_{CA}) on the prediction of budbreak dates (D_{BB}) for two different calibration datasets

Onset of chilling accumulation D_{CA}	Chilling effect	Dataset 1						Dataset 2					
		k	n	Eff	RMSE (days)	AIC_C	RMSEP (days)	n	Eff	RMSE (days)	AIC_C	RMSEP (days)	
Day of year	Positive only	5	41	0.577	8.04	180.9	7.06	39	0.690	6.92	160.9	7.27	
	Positive and negative	7	41	0.568	8.15	186.1	7.25	39	0.659	7.28	168.8	7.88	
Mean temp	Positive only	5	41	0.570	8.10	181.5	7.31	39	0.625	7.69	169.1	7.55	
	Positive and negative	7	41	0.514	8.63	190.7	7.86	39	0.494	8.86	184.1	7.89	
Min temp	Positive only	5	41	0.597	7.85	178.9	7.21	39	0.633	7.58	168.0	7.57	
	Positive and negative	7	41	-1.420	11.36	213.3	12.73	39	-0.274	10.97	200.9	10.00	
First frost	Positive only	4	41	0.381	9.52	192.7	16.29	39	-0.390	14.72	217.7	8.75	
	Positive and negative	6	41	-9.980	40.95	316.4	86.24	39	-33.094	72.30	345.9	10.69	
Photoperiod	Positive only	5	41	0.579	8.01	180.7	6.74	39	0.687	6.94	161.1	7.32	
	Positive and negative	7	41	0.408	9.66	199.9	7.97	39	0.667	7.18	167.8	8.09	
CU_{min} ori	Positive only	4	41	0.173	11.17	205.9	10.88	39	0.439	9.33	182.2	9.27	
	Positive and negative	2	41	-18.955	54.34	331.6	63.04	39	-24.688	63.84	328.2	55.42	
CU_{min} adj	Positive only	8	41	0.585	7.94	185.9	7.48	39	0.609	7.81	176.3	7.66	
	Positive and negative	10	41	0.390	9.80	207.1	9.75	39	0.277	10.29	201.8	10.56	
Leaf fall thermal ori	Positive only	4	41	0.614	7.67	175.0	6.88	39	0.622	7.66	166.8	7.70	
	Positive and negative	6	41	0.606	7.75	179.9	6.76	39	0.653	7.36	167.7	7.41	
Leaf fall thermal adj	Positive only	7	41	0.550	8.30	187.6	6.77	39	0.697	6.84	163.9	7.29	
	Positive and negative	9	41	0.551	8.31	191.6	7.71	39	0.692	6.92	168.9	7.42	
Leaf fall photothermal ori	Positive only	4	41	0.601	7.82	176.6	7.16	39	0.677	7.08	160.7	7.37	
	Positive and negative	6	41	0.638	7.47	176.9	6.68	39	0.684	7.01	163.9	7.18	
Leaf fall photothermal adj	Positive only	7	41	0.636	7.49	179.1	6.82	39	0.685	6.97	165.4	7.23	
	Positive and negative	9	41	-41.417	80.49	377.8	73.53	39	0.671	7.14	171.3	6.94	
DORMPHOT ori	Positive only	4	41	0.611	7.74	175.9	6.89	39	0.671	7.13	161.3	7.63	
	Positive and negative	6	41	0.649	7.39	176.0	6.82	39	0.679	7.05	164.4	7.51	
DORMPHOT adj	Positive only	8	41	0.617	7.67	183.1	6.90	39	0.664	7.28	170.9	7.67	
	Positive and negative	10	41	0.485	8.88	199.1	7.04	39	0.681	7.00	171.8	8.23	

Note: RMSE, RMSEP, and AIC_C lower than 110% of the minimum are indicated in bold. D_{CA} were either fixed (DOY) or computed according to date of first frost (FF), minimum temperature (T_{min}), mean temperature (T_{mean}), photoperiod, minimum chilling unit (CU_{min}), leaf fall using temperature (LFT) or temperature and photoperiod (LFPT), and DORMPHOT (DP). The terms ori and adj refer to the original published version or adjusted to the data, respectively. Chilling effect were only positive, using the reverse Richardson function, or negative at warm temperature, using the smoothed Utah function. k is the number of fitted parameters and n the number of data used to fit the model.

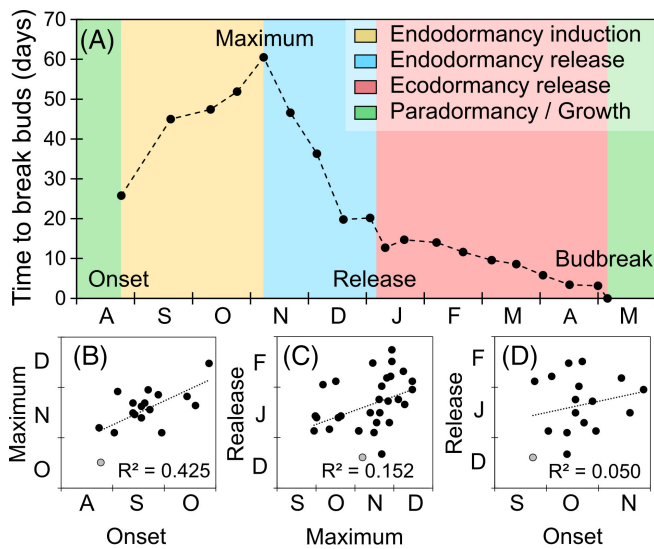


FIGURE 1 (A) Time to break buds under forcing conditions for one node cuttings of *Juglans regia* cv Franquette. Different colors represent the different phenological stages based on the dynamics in time to break buds. The onset of endodormancy, the maximum endodormancy depth, the date of endodormancy release, and the date of budbreak are indicated. (B–D) Correlations between the onset of endodormancy induction, the maximum endodormancy depth, and the date of endodormancy release. The datapoints from the dynamic of panel A are indicated in gray \circ , panels B–D.

3.4 | Predictions under current and future climates for *J. regia* cv Franquette

As shown in the previous section, most of the rules for setting D_{CA} provided relatively accurate phenological predictions for D_{ER} (RMSEP <15 days) and D_{BB} (RMSEP <8 days), except for FF and CU_{\min_ori} . However, the predicted D_{CA} was very different across rules, from late August (Photoperiod) to November (DP_{ori} ; Figure 2A), with Pearson's correlation coefficients r between -0.403 and 0.989 (Table S5). For most of the rules, the average D_{CA} computed across France exhibited close and significant exponential relationships with the mean annual temperature (MAT; $P < 0.001$), except for DOY (defined as a constant; Figure 2B). The D_{CA} predicted by CU_{\min} and FF also exhibited a significant relationship with the mean annual temperature, although through different log-like (or linear) functions (Figure S1).

Despite the large variability in D_{CA} (ca. 60 days difference in the median), the prediction of the D_{ER} was highly reproducible for most rules, in mid-January (Figure 2C), with Pearson's r between 0.875 and 0.999 (Table S6). The relations between D_{ER} and MAT fit exponential functions for all rules ($P < 0.001$), with almost no difference above 7°C . Below this value, three models deviate from the others: LFT_{ori} and $LFPT_{adj}$ predicted earlier endodormancy release dates, whereas later dates for $LFPT_{ori_Utah}$ (Figure 2D). For the budbreak date, predictions were almost identical for all rules with a prediction at the end of April, with Pearson's r between

0.960 and 0.999 (Table S7). The relations between D_{BB} and MAT fit cubic functions and were not distinguishable from each other (Figure 2F). All rules returned a local minimum for MAT between (12.3°C [LFT_{adj}] and 13.5°C [Photoperiod]). This temperature represents a tipping point above which budbreak dates is predicted to be delayed by warmer temperature.

DP_{adj} (positive only) was selected as a representative model to explore current and future phenology trends since this ruled had the highest average performance across 0.597 . D_{CA} , D_{ER} , and D_{BB} have a structured geographical distribution across France (Figure 3). D_{CA} spanned a range of 43 days: earlier in the mountain areas (mid-August) and later on the Mediterranean (South East; late September) and south-western coasts (late August–mid-September). D_{ER} had a similar distribution but over a wider range (84 days): from the beginning of December in mountain areas to the end of February on the Mediterranean coast. D_{BB} showed an opposite distribution over a period of 72 days: from mid-April in the southern and western regions to the end of June in the mountainous areas.

Warmer temperatures, as predicted by the different climate scenario, are therefore expected to delay the onset of chilling accumulation by 5–6 days until 2050 and, by the end of the century, by up to 20 days according to the RCP 8.5 scenario (Figures 4A,G and S2). Endodormancy release is projected to be delayed by a similar magnitude: 6–7 days until 2050 and, by the end of the century, up to 24 days under RCP 8.5 (Figures 4B,H and S3). However, the delay in the release of endodormancy did not directly affect the D_{BB} . The D_{BB} would occur only 3–4 days earlier until 2050 (Figures 4C,I and S4). By the end of the century, budbreak is projected to be earlier under the RCP 4.5 scenario (-6.4 days) than under the warmer RCP 8.5 scenario (-3.5 days).

The relationship between D_{BB} and temperature was not monotonic, exhibiting a tipping point, that is, a temperature above 13.2°C induces later D_{BB} (Figure 2F). In the future climate, the relationships are similar, although the tipping point is slightly shifted toward a warmer temperature: 13.8°C in all scenarios between 2005 and 2050 and up to 14.9°C for the RCP 8.5 scenario (Figure 5C). Finally, a later budbreak than today is likely to occur in larger parts of France at the end of the 21st century: from 5.6 (RCP 4.5) to 33.8% (RCP 8.5) of French territory in 2051–2100 (Figure 6). A similar trend was observed using a fixed date (DOY) to define the onset of chilling accumulation with a tipping point between 13.3°C (current climate) and 14.9°C (RCP 8.5). Using the DOY rule, a later bud break than today is expected in between 4.0 (RCP 4.5) to 30.0% (RCP 8.5) of the French territory in 2051–2100.

The current annual variability of phenological stages is similar for D_{CA} and D_{ER} (standard deviation of about 5 days; Figure 4D,E). The future climate would increase the variance of D_{CA} and D_{ER} considerably, especially for RCP 8.5 in the period 2051–2100 (about 10 days). However, the pattern is reversed for D_{BB} , with a standard deviation of 10 days in the current period, while 5–7 days are expected in the future climate (Figure 5F). In both Protected Designation of Origin (PDO) areas, the variance in D_{BB} would decrease by 2–3 days (RCP 8.5 scenario).

FIGURE 2 Predicted average dates of onset of chilling accumulation (A and B), endodormancy release (C and D) and budbreak (E and F) predicted across France under current climatic conditions using different rules for the onset of chilling accumulation. (A, C, E) The boxes represent the upper and lower quartile with the median indicated by a thick black line, the whiskers represents the 1st and 9th decile, outliers were not represented. (B, D, F) Average dates of onset of chilling accumulation (B), endodormancy release (D), and budbreak (F) depending on mean annual temperature.

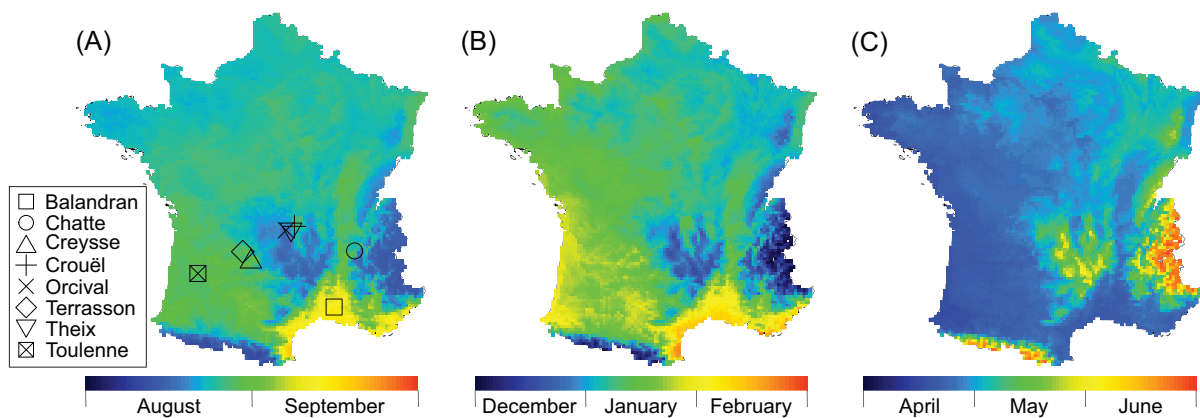
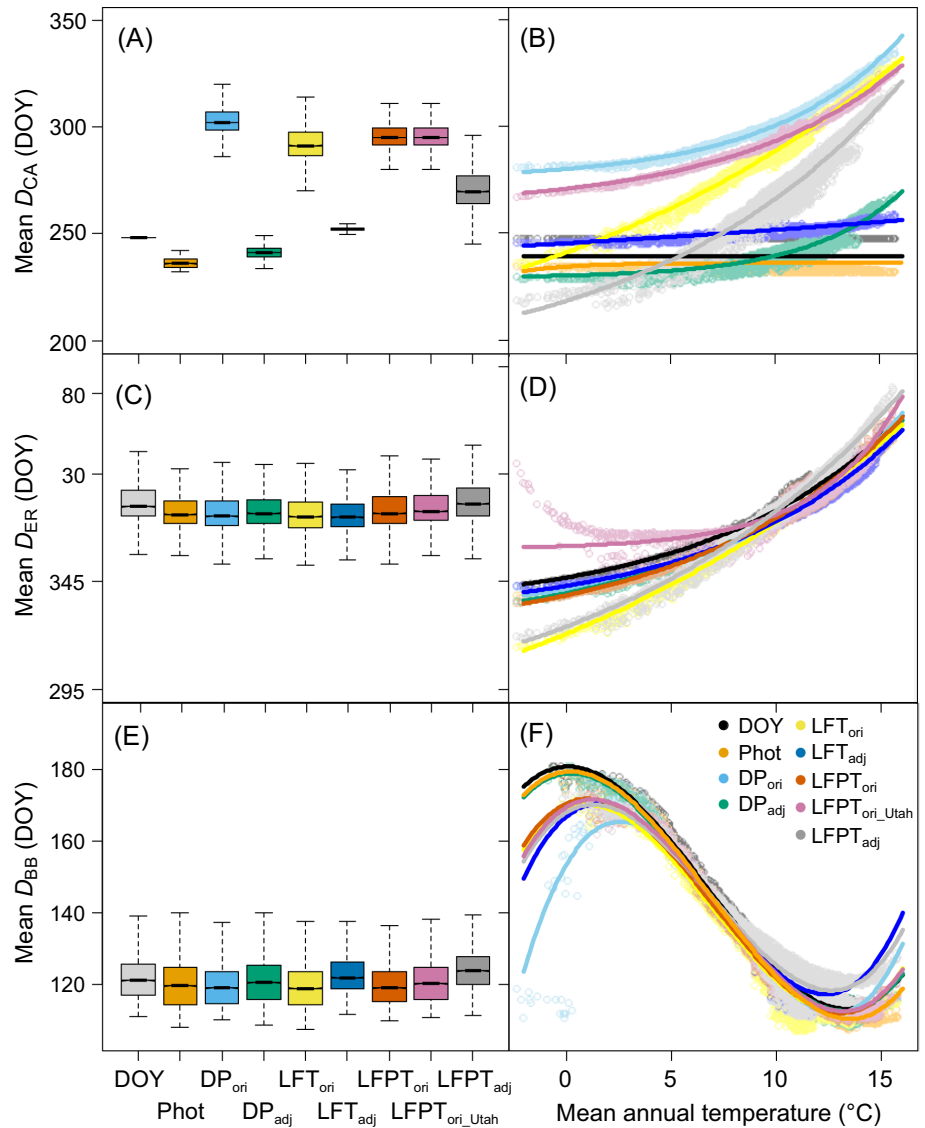


FIGURE 3 Average dates of onset of chilling accumulation D_{CA} (A), endodormancy release D_{ER} (B), and budbreak D_{BB} (C) predicted across France of *Juglans regia* cv Franquette under current climatic conditions using the DORMPHOT model (DP_{adj}).

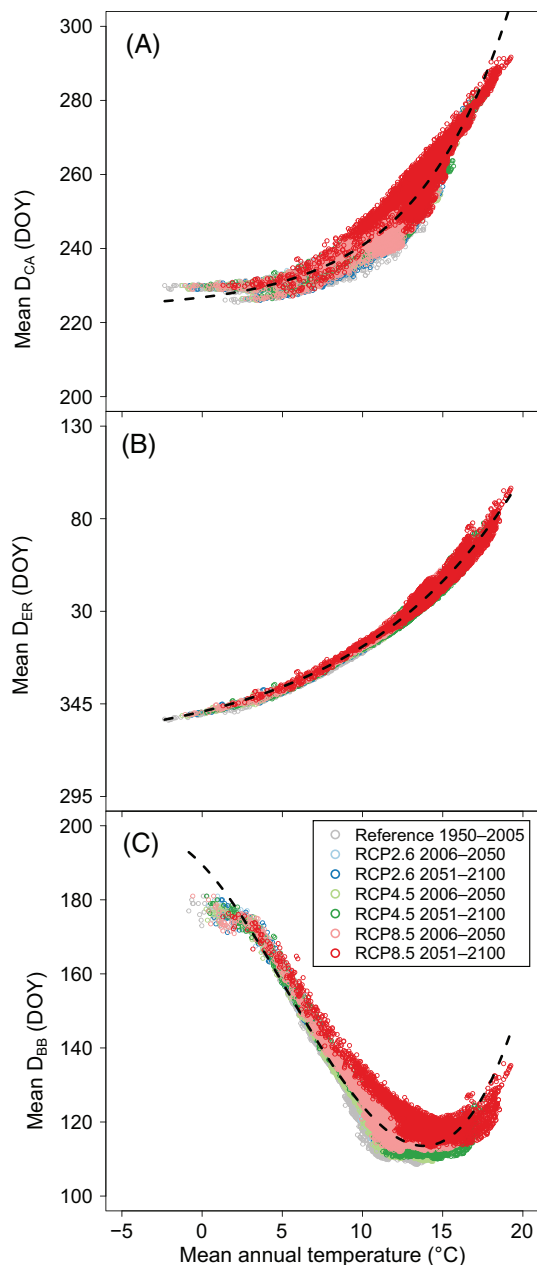


FIGURE 4 Distribution of the mean (A–C) and standard deviation (D and E) in the date of onset of chilling accumulation (A, D), endodormancy release (B, E) and budbreak (C, F) in the current period (Ref) or RCP scenario in the early (2006–2050) and late part of the XXI century (2051–2100) in France. Distribution of the variation compared to the reference period in the mean date of onset of chilling accumulation (G), endodormancy release (H), and budbreak (I). The box represents the upper and lower quartile with the median indicated by a thick black line, the whiskers represents the 1st and 9th decile, outliers were not represented. Different letters indicate a significantly different distribution across scenario according to the non-parametric Kruskal Wallis test ($P < 0.05$).

4 | DISCUSSION

4.1 | Defining the onset of chilling accumulation

The definition of the initial date for the simulation of cyclical processes is a key issue. To predict the annual phenological cycle of

perennial organisms, such as trees, various empirical rules have been used so far. The onset of chilling accumulation during the endodormancy stage (D_{CA}) had, for instance, been arbitrarily set using fixed dates regardless of year and location (Chuine et al., 2016) or based on environmental factors controlling the induction of endodormancy (Caffarra, Donnelly, & Chuine, 2011b). In the current study, long-term observations of phenological stages (endodormancy release D_{ER} and bud break D_{BB}) were used to define the most efficient rule under various environmental conditions. For most of the computations, the different rules for defining the D_{CA} did not have a large impact on the accuracy of the endodormancy release and budbreak dates (ca. 2–3 days; Tables 2 and 3). Overall, the use of a function that computes the negative effect of warm temperature, such as the Utah model, decreased the accuracy of the prediction. The Utah model, developed in *Prunus* does not apply to *Juglans*, as also shown by Chuine et al. (2016).

Across years and sites, the large ranges of variation in dates of endodormancy induction, maximum dormancy and endodormancy release (more than 2 month; Figure 1) suggest that they cannot be predicted by a simple trigger such as a fixed date or photoperiod (Caffarra, Donnelly, Chuine, & Jones, 2011a). Furthermore, the strong correlation between the onset of endodormancy (August–October) and the maximum depth of dormancy (October–December) indicates that the duration of endodormancy induction is generally 2 month with a relatively small effect of environmental conditions (Figure 1). In contrast, the maximum depth of endodormancy and endodormancy release are weakly, although significantly, correlated, with temperature being the main driver of endodormancy release (Weinberger, 1950). However, it is not clear whether chilling temperature actually acts only during endodormancy release or already during the induction of endodormancy.

Model optimization was used to understand the interaction between environmental factors and the induction of endodormancy. Optimization of the different D_{CA} rules led to a wide range of variation in this variable but this was not reflected in the prediction of D_{ER} and D_{BB} (Figure 2). However, not all the rules are effective in predicting D_{ER} and D_{BB} . Among the rules tested, the date of the first frost event and the date of CU_{min} were less effective than the other rules (Tables 2 and 3). Although CU_{min} and FF returned similar average D_{CA} than $LFPT_{adj}$ and DP_{ori} , respectively, their lower ability to predict D_{ER} and D_{BB} suggest a minor role of temperature in setting the date of dormancy induction, as revealed by a different relationship with mean annual temperature (Figure S1). The relevant rules (DOY, DP, LFT, LFPT, and Photoperiod) have indeed considered a potential effect of photoperiod, either directly or indirectly via the fixed date (Chuine & Régnière, 2017; Gauzere et al., 2019; Welling et al., 1997). The LFT, LFPT, and DORMPHOT models, originally developed in *Quercus* sp., *Fagus* sp., and *Betula* sp., are also relevant for other deciduous species such as *Juglans* sp.

The relatively small effect of D_{CA} on D_{ER} and D_{BB} observed here could be the result of various factors such as an inadequacy of the dataset to reflect a wide range of variations in environmental

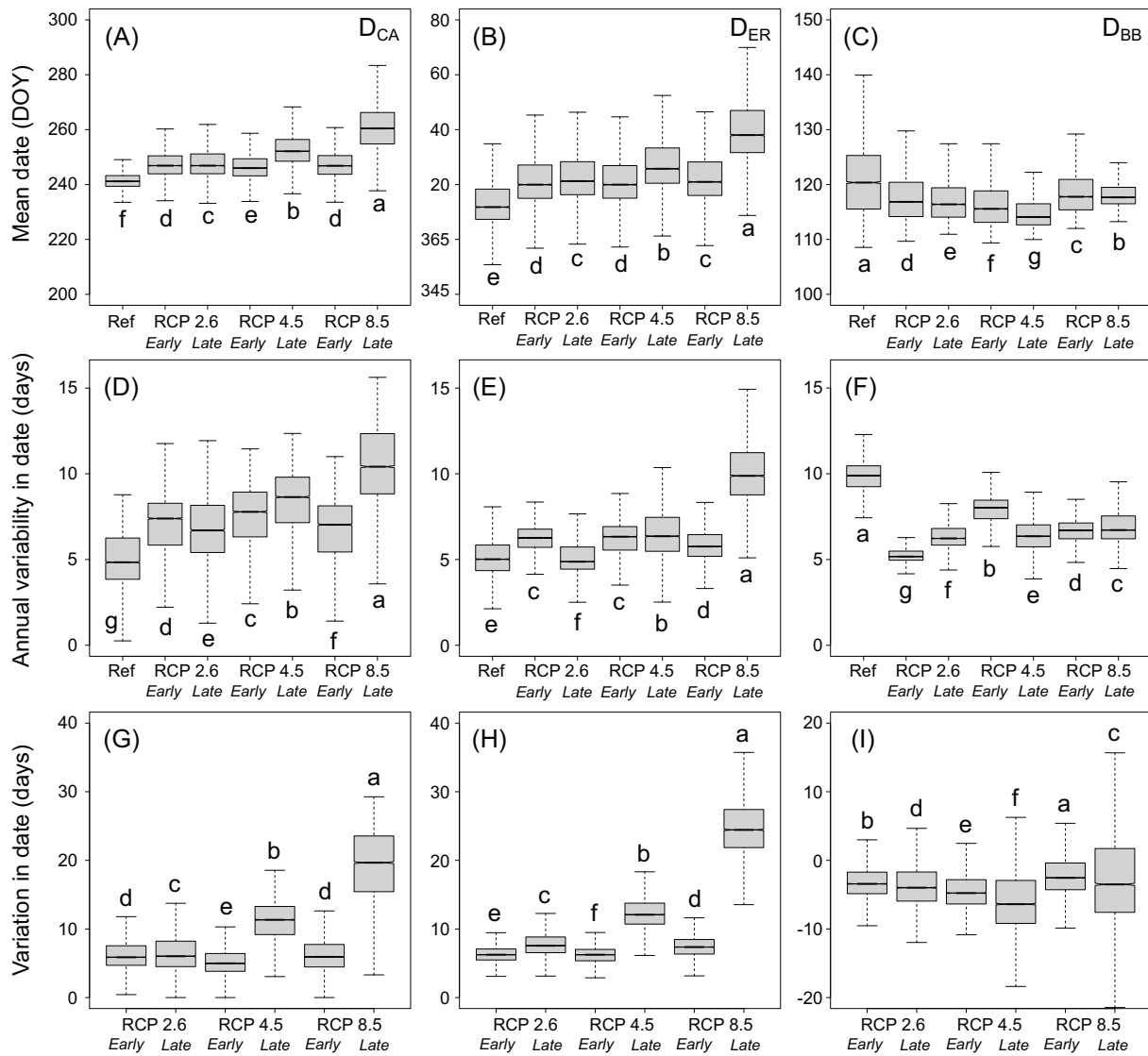


FIGURE 5 (A–C) Average date of onset of chilling accumulation (A), endodormancy release (B), and budbreak (C) depending on mean annual temperature across France under different climatic scenarios using the DORMPHOT model (DP_{adj}). Exponential (A, B) and cubic (C) functions were represented in black dashed lines.

conditions, endodormancy and budbreak dates. However, the calibration dataset was chosen to maximize environmental conditions for the D_{ER} ($MAT = 6.6$ and $14.0^{\circ}C$ for the coldest and warmest year, respectively), and the D_{BB} ($MAT = 6.6$ and $15.0^{\circ}C$). In addition, most of the models were more accurate than the null model: RMSE and RMSEP were lower than the standard deviations for D_{ER} and D_{BB} (15.0 and 10.4 days, respectively). Furthermore, the two calibration procedures were in agreement. To my knowledge, the number of observations (i.e. 38 D_{ER} and 77 D_{BB}) represents the largest dataset combining both phenological stages in the literature. For instance, in the studies cited in Table S1, only one paper combined more than 10 observation of both D_{ER} and D_{BB} (Chuine et al., 2016). According to their conclusions, the model optimization was performed in sequential order as the concomitant fitting of both dates would have given a higher weight to D_{BB} (77 dates) compared to D_{ER} (38 dates) leading to potentially

biased results such as unrealistic dormancy release dates (Chuine et al., 2016).

4.2 | Model optimization versus experimental evidence

Four rules suggest that D_{CA} occurs in early September (DOY, DORMPHOT, LFT, and Photoperiod) whereas the others suggest that D_{CA} occurs in late October (Figure 2), both periods being on the edge of observed onset of endodormancy (Figure 1). All relevant rules integrate the effect of photoperiod, interacting with temperature for some rules. Temperature and photoperiod are closely correlated over the seasons, and it is often difficult to consider their effect independently under natural conditions. As the induction of

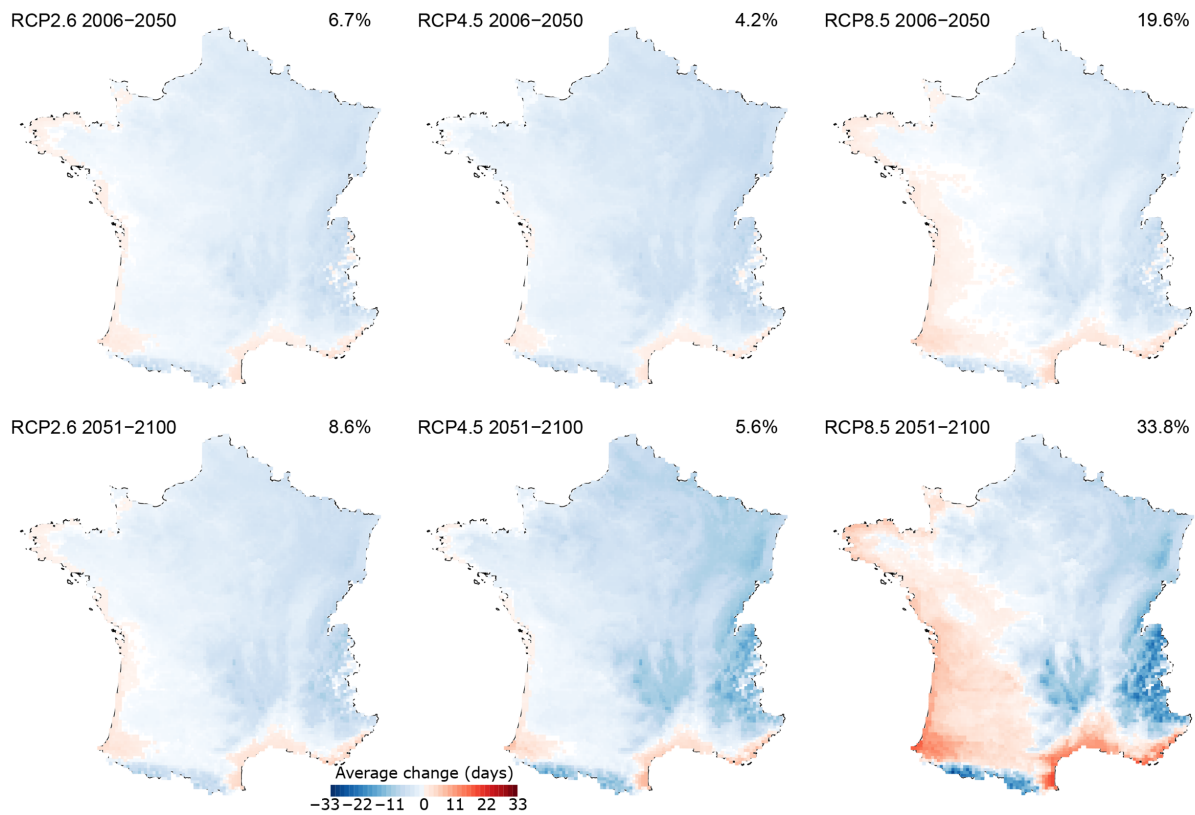


FIGURE 6 Relative change compared to the present period in average budbreak dates across France according to different climatic scenarios (RCP 2.6, RCP 4.5, and RCP 8.5) and time periods (2006–2050 and 2051–2100) using the DORMPHOT model (DP_{adj}). Earlier and later budbreak dates than the current climate are represented in blue and red, respectively. The percentage represent the ratio of the total area that will present delayed budbreak compared to the present time.

endodormancy is a long process (ca. 2 month), perennial plants cannot rely solely on temperature changes that may be too sudden to induce winter dormancy in time (Caffarra, Donnelly, Chuine, & Jones, 2011a). The observations used in this study were performed in different orchards with large differences in MAT (9.7–16.9°C), but at a similar latitude (43.8–45.8° N) with low differences in photoperiod (16 min at solstice). It is therefore difficult to estimate the respective influence of these two factors in *Juglans*. Photoperiod and temperature variables affect the induction of endodormancy of perennial plants, although to different extents across species: photoperiod is dominant in *Populus* (Kalcsits et al., 2009) and *Vitis* (Fennell & Hoover, 1991), whereas temperature is dominant in *Malus*, *Pyrus* (Heide & Prestrud, 2005), and *Sorbus* (Heide, 2011). The interaction between photoperiod and temperature has been demonstrated in *Prunus* (Heide, 2008). In northern plants, Tanino et al. (2010) suggested the existence of two parallel pathways leading buds to dormancy, one under the control of cold temperature and the other under the control of photoperiod. It has been hypothesized that the modulation of photoperiod sensitivity by temperature might be related to the thermal effect on day length perception by phytochromes (Møllmann et al., 2005). The conceptual development of the DORMPHOT model is based on experimental results of dormancy combining the manipulation of photoperiod and

temperature (Caffarra, Donnelly, & Chuine, 2011b), whereas other formalisms were based on empirical observations (e.g. leaf fall; Delpierre et al., 2009).

Finally, it is not possible to conclude whether buds actually integrate chilling information during the budset and the induction of endodormancy because models setting D_{CA} in late summer or in late autumn do not diverge (Figure 2). From a modeling perspective, the use of temperature instead of (or in interaction with) photoperiod can lead to large differences in future climate projections. Delayed induction of endodormancy is likely to have profound consequences for autumn frost risks by delaying or reducing frost acclimation (Charrier, Chuine, et al., 2018a; Guàrdia et al., 2016). The use of experimental results remains essential to ensure that the factors included, and the responses fitted remain realistic (Charrier & Améglio, 2011; Charrier et al., 2018b; Chuine et al., 2016; Hänninen et al., 2019).

4.3 | Predictions across France

Across the different rules, D_{ER} predictions were relatively stable: during January across France. However, three rules diverged from the others at lower temperature than 7°C. $LFPT_{ori_Utah}$ predicts later endodormancy release than the other rules at cold temperature,

probably because the negative chilling units are accumulated in these locations immediately after the D_{CA} . Conversely, LFT_{ori} and $LFPT_{adj}$ predict earlier dormancy than the other rules at cold temperature. The two rules have a significantly higher photoperiod threshold (>14.5 h) than the others, predicting earlier chilling accumulation in cold environment. However, these predictions, outside the calibration range (between 9.7 and 16.9°C; Table 1) should be considered highly putative. Furthermore, stations with mean annual temperature below 7°C represent only 3% of the French territory.

For budbreak, all the different rules provided strikingly similar predictions (Pearson's $r > 0.961$; Table S7). All rules follow a cubic function, revealing a tipping point for D_{BB} at a temperature warmer than 12.3–13.5°C (Figure 2F). Above this threshold, endodormancy release would be more delayed than ecodormancy hastened, resulting in delayed bud break compared to the current period. Under future climate conditions as predicted by the RCP scenarios, the tipping point would be reached in a larger fraction of France. Delayed bud break would thus cover up to one third of France under RCP 8.5 scenario in 2051–2100 using DORMPHOT rule (Figure 6). A similar proportion (30%) would also be observed using a fixed date DOY. The expected delay in D_{BB} in the future climate would therefore be due to insufficient chilling exposure during endodormancy release rather than a delay in D_{CA} . Such a lack of chilling during endodormancy has also been assumed for apricot in the United Kingdom (Martínez-Lüscher et al., 2017) and would be even more exacerbated in subtropical area (Erez, 2000). The tipping point is shifted depending on the scenario (e.g. from 14.1 to 14.9°C, under current and RCP 8.5 in 2051–2100 projections using DOY to set D_{CA}) suggesting that although chilling requirements are delayed, a warmer spring than at present can eventually partly compensate for the induced delay.

Considering the main French production areas, that is, “Noix de Grenoble” (Middle East) and “Noix du Périgord” (Middle West) PDO areas, budbreak would be delayed in most of the “Noix du Périgord” area (96.8% in RCP 8.5 2051–2100) but not in the “Noix de Grenoble” area. These two PDO areas would indeed face distinct threats as they are on opposite sides of the tipping point. In Périgord, chilling requirements are likely not to be fulfilled and varieties with lower chilling requirements should be selected, as current varieties do not exhibit variability for this trait (Charrier et al., 2011). In Grenoble, earlier budbreak dates are expected, leading to greater exposure to late frost events (i.e. vulnerable to false springs) and varieties with higher forcing requirements can help stabilize production (Charrier, Chuine, et al., 2018a).

Interestingly, in the future climate, the annual variability of D_{BB} is expected to be lower. The trend toward more uniform phenology in warm years has already been observed in recent decades for budbreak (Caffarra et al., 2014; Vitasse et al., 2018) and other phenological stages (Stemkovski et al., 2021). It is likely that the response to warm temperature is somewhat saturated with developmental functions reaching a plateau (Caffarra, Donnelly, Chuine, &

Jones, 2011a) and eventually declining at even warmer temperature (Schoolfield et al., 1981). A more uniform phenology would act as a stabilizing factor for fruit production by synchronizing pollination and ripening. However, the lack of chilling temperature during endodormancy induces serious agronomic issues such as erratic patterns of blooming, floribondity, and potential dischronism with anthesis (Campoy et al., 2011).

5 | CONCLUSIONS AND PERSPECTIVES

The modeled approach suggests that the role of D_{CA} is minor in predicting D_{ER} and D_{BB} explaining why many rules have been used for phenological modeling. A stronger role of photoperiod rather than temperature was shown, which is consistent with the experimental results. A tipping point of budbreak dates will probably be reached during the 21st century with chilling requirements likely to be fulfilled later or not at all. An accurate assessment of temperature and photoperiod responses during endodormancy is therefore necessary to complement the experimental data obtained during the ecodormancy stage (Charrier et al., 2011). Although the physiological mechanisms driving the onset of endodormancy may be profoundly altered by global change (Charrier et al., 2021; Hänninen & Tanino, 2011), they appear to have minimal impact on the way current models predict dormancy and bud break dates in walnut.

AUTHOR CONTRIBUTIONS

Data analysis, writing, and editing original manuscript: Guillaume Charrier.

ACKNOWLEDGMENTS

The author wants to acknowledge the essential contribution of Marc Bonhomme, Aline Faure, Jean-Claude Mauget, Remi Rageau, Jean-Pierre Richard for dormancy release date measurements. Phenological data and stem materials were provided by Neus Aleita, Romain Baffoin, Fabrice Lheureux, Marianne Naudin, and Eloise Tranchand. The author is also thankful to Thierry Améglio, André Lacoite, and Heikki Hänninen for constructive comments on preliminary versions of the manuscript. Part of the collected data were supported by the Pôle National de Données de la Biodiversité (a.k.a SOERE Tempo) and by a “Pari Scientifique” grant from the division AgroEcoSystem of INRAE. The author also acknowledges the Auvergne-Rhône-Alpes Region (project Doux-Glace), the French National Research Agency (Acoufollow ANR-20-CE91-008), and the European Union (Life Frostdefend CCA/GR/001747) for financial support.

DATA AVAILABILITY STATEMENT

The data that support the findings of this study are available from the corresponding author upon reasonable request.

ORCID

Guillaume Charrier  <https://orcid.org/0000-0001-8722-8822>

REFERENCES

- Akaike, H. (1974) New look at statistical-model identification. *IEEE Transactions on Automatic Control*, 19, 716–723.
- Arora, R., Rowland, L.J. & Tanino, K. (2003) Induction and release of bud dormancy in woody perennials: a science comes of age. *HortScience*, 38(5), 911–921.
- Balandier, P., Gendraud, M., Rageau, R., Bonhomme, M., Richard, J.P. & Parisot, E. (1993) Bud break delay on single node cuttings and bud capacity for nucleotide accumulation as parameters for endo- and paradormancy in peach trees in a tropical climate. *Scientia Horticulturae*, 55(3–4), 249–261.
- Basler, D. & Körner, C. (2012) Photoperiod sensitivity of bud burst in 14 temperate forest tree species. *Agricultural and Forest Meteorology*, 165, 73–81.
- Beauvieux, R., Wenden, B. & Dirlwanger, E. (2018) Bud dormancy in perennial fruit tree species: a pivotal role for oxidative cues. *Frontiers in Plant Science*, 9, 657.
- Beil, I., Kreyling, J., Meyer, C., Lemcke, N. & Malyshev, A.V. (2021) Late to bed, late to rise—warmer autumn temperatures delay spring phenology by delaying dormancy. *Global Change Biology*, 27(22), 5806–5817.
- Bonhomme, M., Rageau, R. & Lacoïnte, A. (2007) Optimization of endodormancy release models using series of endodormancy release data collected in France. *Acta Horticulturae*, 872, 51–60.
- Caffarra, A., Donnelly, A., Chuine, I. & Jones, M.B. (2011a) Modelling the timing of *Betula pubescens* budburst. I. Temperature and photoperiod: a conceptual model. *Climate Research*, 46(2), 147–157.
- Caffarra, A., Donnelly, A. & Chuine, I. (2011b) Modelling the timing of *Betula pubescens* budburst. II. Integrating complex effects of photoperiod into process-based models. *Climate Research*, 46(2), 159–170.
- Caffarra, A., Zottele, F., Gleeson, E. & Donnelly, A. (2014) Spatial heterogeneity in the timing of birch budburst in response to future climate warming in Ireland. *International Journal of Biometeorology*, 58(4), 509–519.
- Campoy, J.A., Ruiz, D. & Egea, J. (2011) Dormancy in temperate fruit trees in a global warming context: a review. *Scientia Horticulturae*, 130(2), 357–372.
- Charrier, G. & Améglio, T. (2011) The timing of leaf fall affects cold acclimation by interactions with air temperature through water and carbohydrate contents. *Environmental and Experimental Botany*, 72(3), 351–357.
- Charrier, G., Bonhomme, M., Lacoïnte, A. & Améglio, T. (2011) Are budburst dates, dormancy and cold acclimation in walnut trees (*Juglans regia* L.) under mainly genotypic or environmental control? *International Journal of Biometeorology*, 55(6), 763–774.
- Charrier, G., Ngao, J., Saudreau, M. & Améglio, T. (2015) Effects of environmental factors and management practices on microclimate, winter physiology, and frost resistance in trees. *Frontiers in Plant Science*, 6, 259.
- Charrier, G., Chuine, I., Bonhomme, M. & Améglio, T. (2018a) Assessing frost damages using dynamic models in walnut trees: exposure rather than vulnerability controls frost risks. *Plant, Cell & Environment*, 41(5), 1008–1021.
- Charrier, G., Lacoïnte, A. & Améglio, T. (2018b) Dynamic modeling of carbon metabolism during the dormant period accurately predicts the changes in frost hardiness in walnut trees *Juglans regia* L. *Frontiers in Plant Science*, 9, 1746.
- Charrier, G., Martin-Stpaul, N., Damesin, C., Delpierre, N., Hänninen, H., Torres-Ruiz, J.M. et al. (2021) Interaction of drought and frost in tree ecophysiology: rethinking the timing of risks. *Annals of Forest Science*, 78(2), 1–15.
- Chuine, I. & Régnière, J. (2017) Process-based models of phenology for plants and animals. *Annual Review of Ecology, Evolution, and Systematics*, 48, 159–182.
- Chuine, I., Bonhomme, M., Legave, J.M., García de Cortázar-Atauri, I., Charrier, G., Lacoïnte, A. et al. (2016) Can phenological models predict tree phenology accurately in the future? The unrevealed hurdle of endodormancy break. *Global Change Biology*, 22(10), 3444–3460.
- Delpierre, N., Dufrière, E., Soudani, K., Ulrich, E., Cecchini, S., Boé, J. et al. (2009) Modelling interannual and spatial variability of leaf senescence for three deciduous tree species in France. *Agricultural and Forest Meteorology*, 149(6–7), 938–948.
- Dennis, F.G. (2003) Problems in standardizing methods for evaluating the chilling requirements for the breaking of dormancy in buds of woody plants. *HortScience*, 38(3), 347–350.
- Déqué, M., Rowell, D.P., Lüthi, D., Giorgi, F., Christensen, J.H., Rockel, B. et al. (2007) An intercomparison of regional climate simulations for Europe: assessing uncertainties in model projections. *Climatic Change*, 81(1), 53–70.
- Erez, A. (2000) Bud dormancy; phenomenon, problems and solutions in the tropics and subtropics. In: *Temperate fruit crops in warm climates*. Dordrecht: Springer, pp. 17–48.
- Faust, M., Erez, A., Rowland, L.J., Wang, S.Y. & Norman, H.A. (1997) Bud dormancy in perennial fruit trees: physiological basis for dormancy induction, maintenance, and release. *HortScience*, 32(4), 623–629.
- Fennell, A., & Hoover, E. (1991) Photoperiod influences growth, bud dormancy, and cold acclimation in *Vitis labruscana* and *V. riparia*. *Journal of the American Society for Horticultural Science*, 116(2), 270–273.
- Gauzere, J., Lucas, C., Ronce, O., Davi, H. & Chuine, I. (2019) Sensitivity analysis of tree phenology models reveals increasing sensitivity of their predictions to winter chilling temperature and photoperiod with warming climate. *Ecological Modelling*, 411, 108805.
- Guàrdia, M., Charrier, G., Vilanova, A., Savé, R., Améglio, T. & Aletà, N. (2016) Genetics of frost hardiness in *Juglans regia* L. and relationship with growth and phenology. *Tree Genetics & Genomes*, 12(5), 1–10.
- Hänninen, H. & Tanino, K. (2011) Tree seasonality in a warming climate. *Trends in Plant Science*, 16(8), 412–416.
- Hänninen, H., Kramer, K., Tanino, K., Zhang, R., Wu, J. & Fu, Y.H. (2019) Experiments are necessary in process-based tree phenology modelling. *Trends in Plant Science*, 24(3), 199–209.
- Heide, O.M. (2008) Interaction of photoperiod and temperature in the control of growth and dormancy of *Prunus* species. *Scientia Horticulturae*, 115(3), 309–314.
- Heide, O.M. (2011) Temperature rather than photoperiod controls growth cessation and dormancy in *Sorbus* species. *Journal of Experimental Botany*, 62(15), 5397–5404.
- Heide, O.M. & Prestrud, A.K. (2005) Low temperature, but not photoperiod, controls growth cessation and dormancy induction and release in apple and pear. *Tree Physiology*, 25(1), 109–114.
- Horvath, D.P., Anderson, J.V., Chao, W.S. & Foley, M.E. (2003) Knowing when to grow: signals regulating bud dormancy. *Trends in Plant Science*, 8(11), 534–540.
- Kalcsits, L.A., Silim, S. & Tanino, K. (2009) Warm temperature accelerates short photoperiod-induced growth cessation and dormancy induction in hybrid poplar (*Populus* × spp.). *Trees*, 23(5), 971–979.
- Lang, G.A., Early, J.D., Martin, G.C. & Darnell, R.L. (1987) Endo-, para-, and ecodormancy: physiological terminology and classification for dormancy research. *HortScience*, 22(3), 371–377.
- Luedeling, E. (2019) *Statistical methods for phenology analysis in temperate fruit trees*. chillR Package.
- Martínez-Lüscher, J., Hadley, P., Ordidge, M., Xu, X. & Luedeling, E. (2017) Delayed chilling appears to counteract flowering advances of apricot in southern UK. *Agricultural and Forest Meteorology*, 237, 209–218.
- Mauget, J.C. (1980) Dormance et précocité de débournement des bourgeons chez quelques cultivars de Noyer (*Juglans regia* L.). *Comptes-rendus de l'Académie des Sciences de Paris D*, 290, 135–138.
- Maurya, J.P. & Bhalerao, R.P. (2017) Photoperiod-and temperature-mediated control of growth cessation and dormancy in trees: a molecular perspective. *Annals of Botany*, 120(3), 351–360.
- Meier, U. (2001) *Growth stages of mono- and dicotyledonous plants*. BBCH Monograph. <https://doi.org/10.5073/bbch0515>

- Mølmann, J.A., Asante, D.K., Jensen, J.B., Krane, M.N., Ernstsen, A., Junttila, O. et al. (2005) Low night temperature and inhibition of gibberellin biosynthesis override phytochrome action and induce bud set and cold acclimation, but not dormancy in PHYA overexpressors and wild-type of hybrid aspen. *Plant, Cell & Environment*, 28(12), 1579–1588.
- Pagter, M., Andersen, U.B. & Andersen, L. (2015) Winter warming delays dormancy release, advances budburst, alters carbohydrate metabolism and reduces yield in a temperate shrub. *AoB Plants*, 7, plv024. <https://doi.org/10.1093/aobpla/plv024>
- R Development Core Team. (2019) *R: a language and environment for statistical computing*. Available at: <https://www.r-project.org/>
- Rageau, R. (1982) Etude expérimentale des lois d'action de la température sur la croissance des bourgeons floraux du pêcher (*Prunus persica* L. Batsch) pendant la postdormance. *Comptes rendus de l'Académie d'Agriculture de France*, 68, 709–718.
- Réaumur, R.A.F.D. (1735) *Observations du thermomètre, faites à Paris durant l'année 1735, comparées avec celles qui ont été faites sous la ligne, à l'isle de France, à Alger et quelques unes de nos isles de l'Amérique*. Mémoires de l'Académie des Sciences de Paris.
- Richardson, E.A., Seeley, S.D. & Walker, D.R. (1974) A model for estimating the completion of rest for “Redhaven” and “Elberta” peach trees. *HortScience*, 9(4), 331–332.
- Rinne, P.L., Kaikuranta, P.M. & Van Der Schoot, C. (2001) The shoot apical meristem restores its symplasmic organization during chilling-induced release from dormancy. *The Plant Journal*, 26(3), 249–264.
- Schoolfield, R.M., Sharpe, P.J.H. & Magnuson, C.E. (1981) Non-linear regression of biological temperature-dependent rate models based on absolute reaction-rate theory. *Journal of Theoretical Biology*, 88(4), 719–731.
- Stemkovski, M., Bell, J.R., Ellwood, E.R., Inouye, B.D., Kobori, H., Lee, S. D. et al. (2021) Disorder or a new order: how climate change affects phenological variability. *bioRxiv*. <https://doi.org/10.1101/2021.10.08.463688>
- Tanino, K.K., Kalcsits, L., Silim, S., Kendall, E., & Gray, G.R. (2010) Temperature-driven plasticity in growth cessation and dormancy development in deciduous woody plants: a working hypothesis suggesting how molecular and cellular function is affected by temperature during dormancy induction. *Plant molecular biology*, 73(1), 49–65.
- Vegis, A. (1964) Dormancy in higher plants. *Annual Review of Plant Physiology*, 15(1), 185–224.
- Vitasse, Y., Signarbieux, C. & Fu, Y.H. (2018) Global warming leads to more uniform spring phenology across elevations. *Proceedings of the National Academy of Sciences*, 115(5), 1004–1008.
- Weinberger, J.H. (1950) Chilling requirements of peach varieties. In: *Proceedings of the American Society for Horticultural Science*, Vol. 56, pp. 122–128. https://scholar.google.com/scholar_lookup?title=Chilling+requirements+of+peach+varieties&author=Weinberger,+J.H.&publication_year=1950&journal=Proc.+Am.+Soc.+Hortic.+Sci.&volume=56&pages=122%E2%80%93128
- Weinberger, J.H. (1956) Prolonged dormancy trouble in peaches in the southeast in relation to winter temperatures. *Journal of the American Society for Horticultural Science*, 6(7), 107–112.
- Weinberger, J.H. (1967) Some temperature relations in natural breaking of the rest of peach flower buds in the San Joaquin Valley, California. *Proceedings of the American Society for Horticultural Science*, 51, 84–89.
- Welling, A., Kaikuranta, P. & Rinne, P. (1997) Photoperiodic induction of dormancy and freezing tolerance in *Betula pubescens*. Involvement of ABA and dehydrins. *Physiologia Plantarum*, 100(1), 119–125.
- Welling, A., Moritz, T., Palva, E.T. & Junttila, O. (2002) Independent activation of cold acclimation by low temperature and short photoperiod in hybrid aspen. *Plant Physiology*, 129(4), 1633–1641.

SUPPORTING INFORMATION

Additional supporting information may be found in the online version of the article at the publisher's website.

How to cite this article: Charrier, G. (2022) Is winter coming? Minor effect of the onset of chilling accumulation on the prediction of endodormancy release and budbreak. *Physiologia Plantarum*, 174(3), e13699. Available from: <https://doi.org/10.1111/ppl.13699>